Optical Microscopy Beyond the Diffraction Limit: Imaging Guided and Propagating Fields

M. Selim Ünlü, Bennett B. Goldberg, and Stephen B. Ippolito

Boston University
Department of Electrical and Computer Engineering
Department of Physics
Photonics Center
8 Saint Mary's St., Boston, MA 02215, USA

ABSTRACT. Diffraction limits standard optical microscopy to a spatial resolution of about half the wavelength of light. We present novel microscopy techniques for imaging semiconductor materials and devices at better than diffraction-limited spatial resolution and observe previously inaccessible phenomena. We discuss the methods and results for Numerical Aperture Increasing Lens (NAIL) and Near-field Scanning Optical Microscopy (NSOM) techniques.

Introduction

There are fundamental limitations of conventional microscopy. In case of imaging objects with optical fields propagating to the far-field, the basic constraint is the diffraction of light, which limits standard optical microscopy to a spatial resolution comparable to the wavelength of light. For imaging objects through a substrate, which is opaque for short wavelengths, this limitation becomes more stringent. Imaging guided-wave devices represents even a bigger challenge for conventional microscopy. In this case, light does not couple to the far-field rendering conventional microscopy useless. In this paper, we discuss several microscopy techniques to overcome the limitations of conventional microscopy. We describe a novel subsurface imaging technique utilizing a Numerical Aperture Increasing Lens (NAIL) [1,2] and its application to Si Integrated Circuits (IC). We also present results on Near-field Scanning Optical Microscopy (NSOM) applied to imaging the beam and divergence properties of laser diodes [3,4,5] and internal fields of Integrated Optical (IO) devices [6,7].

Diffraction limits standard optical microscopy to a spatial resolution of about half the wavelength of light. Figure 1 shows schematically how a conventional lens focuses a collimated beam. In the simplified ideal case of incoming beam size matching the diameter of the lens the minimum spot size at the focal point can be expressed as:

$$2w_{02} \approx \frac{2l}{p\mathrm{NA}} = \frac{l}{n}\frac{4}{p} f_{\#}$$

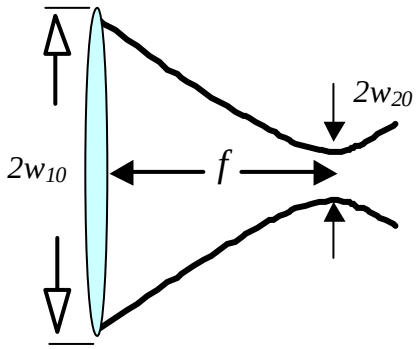

Fig. 1. Schematic representation of how a collimated beam is focused by a converging lens.

where, the *NA* (Numerical Aperture) is $n \times sin\theta$, where n is the refractive index in the object space and θ is the half-angle subtended. The free space wavelength is denoted as λ in the equation. A higher resolution can be obtained by using shorter wavelengths similar to the use of short-wavelength optical lithography for semiconductor circuit fabrication. In most microscopy applications, however, the wavelength cannot be arbitrarily selected. In imaging light emission from materials and devices, wavelength is determined by the material system. In case of imaging through a substrate the wavelength is determined according to the absorption properties. For example, optical absorption in Si limits inspection through the substrate to $\lambda \geq 1$ µm, yielding a theoretical lateral spatial resolution limit for standard subsurface microscopy of ~0.5 µm.

High-resolution Subsurface Microscopy

Current Si integrated circuit (IC) technology includes many opaque metal layers and structures above semiconductor devices, thereby hindering topside inspection of devices in their final state. Hence, inspection through the backside or substrate of a Si IC is often preferred [8]. However, optical absorption in Si limits inspection through the substrate to near infrared wavelengths, yielding a typical lateral spatial resolution values for commercial systems at about 1 µm. In contrast, modern Si IC technology has reached process size scales of 0.13 µm, clearly beyond the capability of standard subsurface microscopy.

Reducing the wavelength or increasing the collected solid angle can improve the spatial resolution of surface microscopy. This has been achieved both with oil immersion and solid immersion lens (SIL) microscopy techniques, [9,10] which reduce the wavelength by immersing the object space in a material with a high refractive index. However, in subsurface microscopy the only method to improve the spatial resolution is to increase the collected solid angle, i.e., the *NA* must be increased. The large *n* in the object space in standard subsurface microscopy of planar samples does not increase the *NA* because of refraction at the planar boundary. The Numerical Aperture Increasing Lens (NAIL) is placed on the surface of a sample as illustrated in Fig. 2 introducing a convex surface and effectively transforming the planar sample into an integrated solid immersion lens. Ideally the NAIL is made of the same material as the sample, in this case Si, both polished to allow intimate contact to avoid reflections at the planar interface. The convex surface of the NAIL is spherical with a radius of curvature of *R*. Light passes through the sample and NAIL from an object space in the sample at a vertical depth of *X*. To increase the *NA* without introducing an additional spherical aberration, the vertical thickness of the lens is selected to be $D = R\times(1+1/n) - X$. In this case the object space coincides with the aplanatic points of the NAIL's spherical surface.

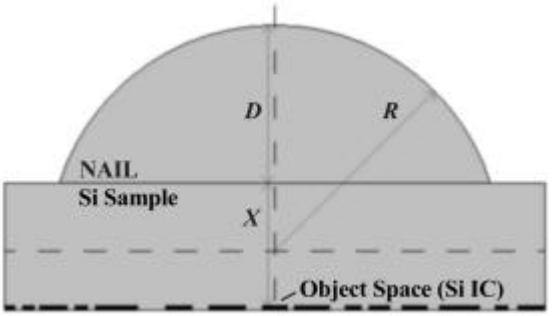

Fig. 2. Schematic representation of NAIL and sample parameters where *D* is the vertical thickness of the NAIL, *R* is the radius of curvature of the NAIL's spherical surface, and *X* is the vertical depth of the sample.

Addition of the NAIL to a standard microscope increases the *NA* by a factor of n^2, up to $NA = n$. In Si, the *NA* is increased by a factor of 13, up to $NA = 3.6$. The *NA* increase also allows for the use of a smaller *NA* microscope objective lens without sacrificing the spatial resolution of the NAIL microscope. A microscope objective lens with $NA = 0.3$ is sufficient to achieve the highest spatial resolution for a Si NAIL microscope. Figure 3 shows images of a SRAM chip fabricated by a 0.18-µm process, displaying the striking improvement provided by the NAIL technique. Features otherwise not visible can be clearly discerned using the NAIL technique. Using a confocal system we demonstrated lateral spatial resolution of approximately 0.2 µm and the theoretical limit is 0.14 µm.

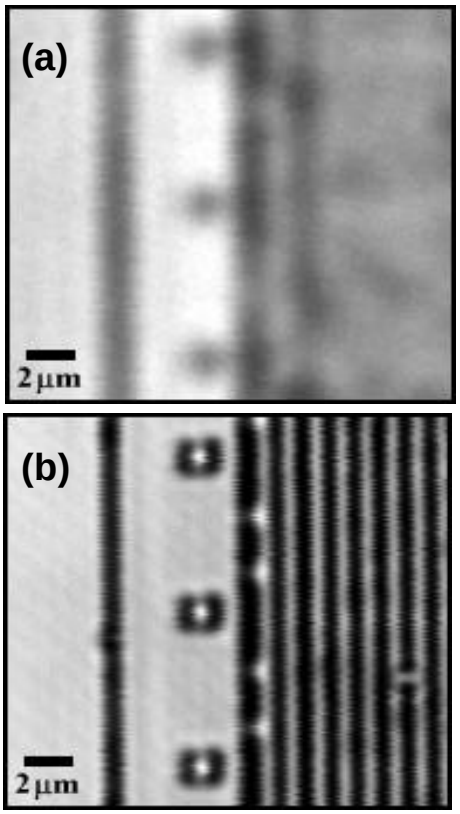

Fig. 3. Images taken by Hamamatsu µAMOS-200, IC Failure Analysis System, demonstrate how a NAIL improves resolution well beyond the state-of-the-art in through-the-substrate imaging of Si circuits. (a) Image obtained using the 100X objective having NA=0.5 and (b) image with the 10X objective (NA=0.25) and NAIL increasing the NA to 3.3.

Near-field Scanning Optical Microscopy of Optoelectronic Devices

Near-field optical microscopy and spectroscopy has emerged as a powerful tool for the investigation of semiconductor structures. In NSOM a tapered optical fiber probe is placed within a fraction of a wavelength of a sample and scanned over the surface [11,12,13]. The tapered single-mode optical fiber provides a tiny aperture through which the light is coupled. Because both the tip-to-sample separation and the tip aperture are a small fraction of the wavelength, the spatial resolution is given approximately by the tip diameter providing a significant improvement. Recent NSOM studies have addressed issue of laser diode mode profiling, minority carrier transport, near-field photocurrent response of quantum well structures and laser diodes, imaging of local waveguide properties, and location and studies of dislocations in semiconductor thin films [3,14].

NSOM of Guided-wave Devices: While accurate simulations of complicated guided-wave devices rely on assumptions about the physical structure, direct measurement of internal optical modes and the local properties of guided-wave propagation have remained elusive. By using a NSOM as a local probe technique, the evanescent field above the waveguide can be measured, providing a detailed and complete picture of the operation of the guided mode, far surpassing previous indirect imaging techniques. Our NSOM measurements profiled internal field intensities and allowed for the determination of all components of the propagation vector [7].

The NSOM probe is scanned over the surface of the waveguide, routing the collected light to a photodetector (Fig. 4). Translation stages used to scan the tip are calibrated to ±0.3 nm by interferometry and a shear-force tuning fork method [15] is used during surface scans to maintain a tip-surface separation of 10 nm.

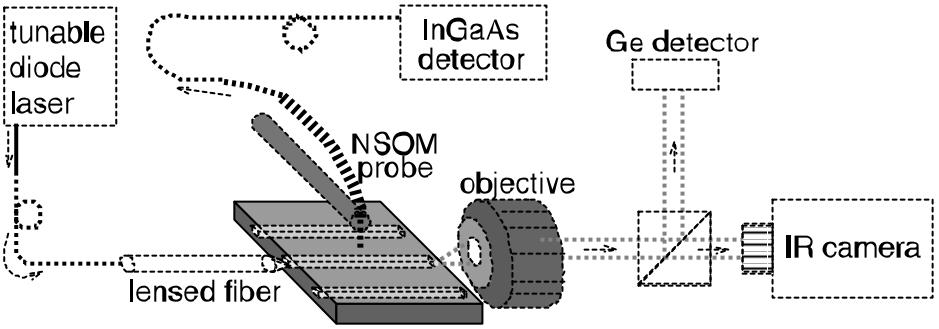

Fig 4. Experimental setup used for characterizing internal optical fields inside guided-wave devices. Light from tunable laser is launched into the device under test, and the transmitted light is analyzed. The NSOM probe is scanned over the surface of the device, measuring both topography and sampling the evanescent field.

The field at the waveguide surface will not be simply related to the internal modes if a large amount of scattering is present. Therefore, a vital initial measurement in this and similar studies is a comparison of the level of scattered light to that of evanescent field at the surface. The measured optical intensity from NSOM scans in the vertical plane, perpendicular to the direction of light propagation, is plotted in Fig. 5(a) on top of the schematic of the structure. The intensity decays quickly as a function of height showing the absence of scattering into free-space propagating modes. This scan also shows

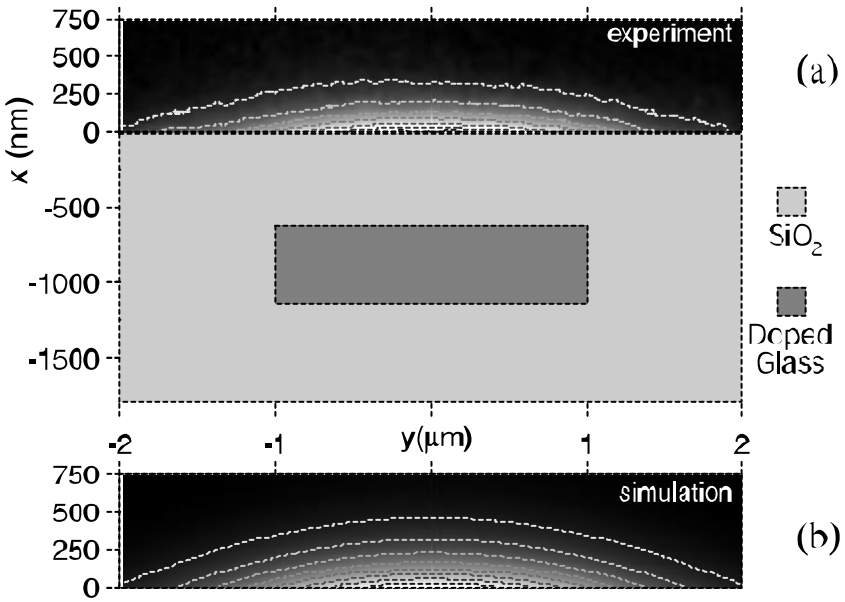

Fig 5. (a) Measured optical intensity from NSOM scans in the vertical plane, shown on top of a cross section of the waveguides under study. Grayscale map uses black to indicate zero intensity, and white for high intensity. Contours are added to enhance visibility of features. A complete decay of the field at a height (x) of around 500nm is observed. (b) Simulation of mode intensity in the same region.

excellent qualitative agreement with the top section of the mode solver simulation, shown in Fig 5(b). A vertical line-cut of this data shows a pure exponential decay consistent with theoretical predictions.

Figure 6 shows a NSOM image obtained by scanning on the surface of the waveguide structure. The dependence along $\hat{y}$ of the measured optical intensity is consistent with a single mode waveguide. The periodic variation in the $\hat{z}$ direction is the standing wave due to the cavity formed between the entrance and exit facets of the waveguide. The period of the standing mode is given by $\lambda_0/2n_{eff}$, where λ_0 is the vacuum wavelength and n_{eff} is the effective index for the guided optical mode. At λ_0 = 1.549µm, the measured n_{eff} = 1.458 compares very favorably with simulations which yield n_{eff}= 1.473. Therefore, measurements of the period of the observed standing modes provides an accurate and direct measure of the effective index, which combined with the measured transverse modal shape and decay constants, determines the values of all spatial components of the wave vector.

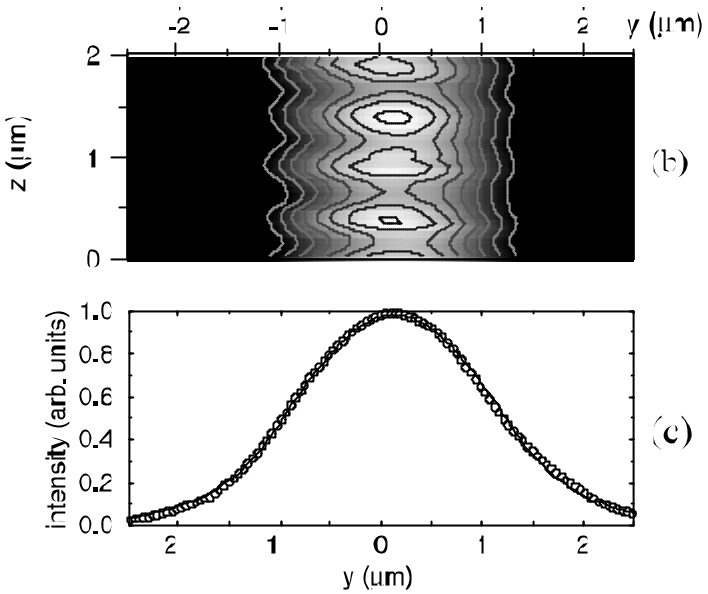

Fig 6. (a) Optical image obtained at the surface of the waveguide when TM modes are excited. The periodic variation in the *z* direction is a standing mode due to a cavity formed in the waveguide. A line cut for *y*=0 exhibits almost pure sinusoidal behavior, with a peak-to-valley ratio of 1.2. (b) Line-cut for constant *z*, with a fit to the lowest order solution in a step-index waveguide.

NSOM of Laser Diodes: We have also studied the beam properties of high power semiconductor lasers using NSOM. In this case, the advantage of NSOM is to provide a means for localized high-resolution sensing of the propagating fields. The laser diodes we tested are designed to emit a nearly diffraction limited single lobe at 980 nm wavelength to be used for optical pumping of erbium doped fiber amplifiers. The resolution capability of conventional microscopy does not allow for a detailed measurement of the beam properties. By scanning an NSOM tip at a constant height from the laser facet the beam profile can be obtained with approximately 100-nm resolution. Figure 7 shows a series of images of the laser mode intensity collected with the NSOM probe as a function of height above the laser facet. Each successive image is 1 µm further from the facet, starting at the immediate vicinity of the surface and ending at 7 µm. Through these measurements it is possible to reconstruct the true near-field beam profile of the laser diode and determine how the beam is oriented with respect to the device. Using this technique we measured astigmatism in laser diodes [4], and studied the beam-steering associated with the kink in the L-I curve [5]. By providing previously inaccessible detail, NSOM allowed us to demonstrate that the previous theory to explain the origin of the non-linearity of the LI curve was not accurate.

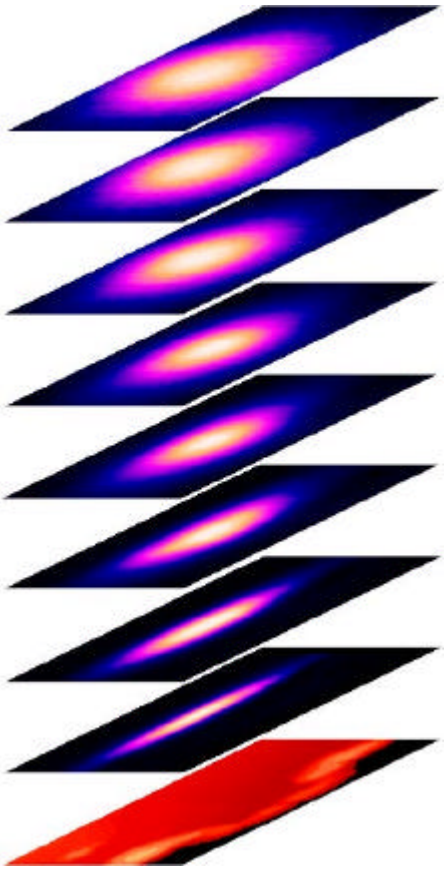

Fig 7. Images (6 µm x 6 µm) of the beam propagation from the near field to 7µm from the facet taken in 1 µm steps. The bottom image is the topography to provide the physical orientation.

Conclusions

In this paper, we presented high-resolution microscopy techniques to study semiconductor materials and devices. These techniques provide lateral resolution well beyond the conventional state-of-the-art and allow for studying structures and phenomena that were not previously accessible. The NAIL subsurface microscopy technique we describe significantly increases the *NA* without introducing an additional spherical aberration. Using the NAIL technique in the near infrared inspection of a Si IC, the theoretical lateral spatial resolution limit is improved to 0.14 µm with preliminary experiments yielding a resolution of better than 0.23 µm. We also demonstrated the use of NSOM in imaging internal spatial modes in glass/silica buried waveguides. We have shown that measurements of the period of the observed standing modes provides an accurate and direct measure of the effective index, which combined with the measured transverse modal shape and decay constants, determines the values of all spatial components of the wave vector. Imaging the beam properties of 980-nm high-power laser diodes by NSOM provided high-resolution images of the mode shape, a direct measurement of astigmatism and shed new light on the understanding of the non-linearity in the L-I characteristics.

References

[1] S. B. Ippolito, B. B. Goldberg, and M. S. Ünlü, "High-resolution Subsurface Microscopy Technique," *Appl. Phys. Lett*., Vol. 78(26), pp. 4071-4073 (2001).

[2] S. B. Ippolito, A. K. Swan, B. B. Goldberg, and M. S. Ünlü, "High-resolution IC Inspection: Through the Substrate Imaging at 0.14 µm Resolution," *SPIE Photonics West*, San Jose, CA, January 2001.

[3] B. B. Goldberg, M. S. Ünlü, W. D. Herzog, and E. Towe, "Near Field Optical Microscopy and Spectroscopy of Heterostructures and Laser Diodes," *IEEE J. Selected Topics in Quantum Electron*. on Applied Optical Diagnostics of Semiconductors, Vol. 1, pp. 1073-1081 (1995). (invited)

[4] W. D. Herzog, M. S. Ünlü, B. B. Goldberg, G. H. Rhodes, and C. Harder, "Beam Divergence and Waist Measurements of Laser Diodes by Near-field Scanning Optical Microscopy," *Appl. Phys. Lett*., Vol. 70(6), pp. 688-690, (1997).

[5] W. D. Herzog, B. B. Goldberg, and M. S. Ünlü, "Beam Steering in High-power 980 nm Laser Diodes," *IEEE Photon. Technol. Lett*., Vol. 12(12), pp. 1604-1606, (2000).

[6] G. H. Vander Rhodes, B. B. Goldberg, M. S. Ünlü, B. Little, S. T. Chu, W. Pan, T. Kaneko, and Y. Kokobun, "Measurement of Internal Spatial Modes and Local Propagation Properties in Optical Waveguides," *Appl. Phys. Lett*., vol. 75, no. 16, pp. 2368-2370, (1999).

[7]G. H. Vander Rhodes, B. B. Goldberg, M. S. Ünlü, S. T. Chu, and B. Little, "Measurement of Internal Spatial Modes in Microring Resonators," *IEEE J. Selected Topics in Quantum Electron*., vol. 6, pp. 1077-1084, (2000).

[8] Instruments of Hamamatsu Corp., 360 Foothill Rd, Bridgewater, NJ 08807, http://www.hamamatsu.com.

[9] B. D. Terris, H. J. Mamin, D. Rugar, W. R. Studenmund, and G. S. Kino, *Appl. Phys. Lett*. 65, 388 (1994).

[10] K. Karrai, X. Lorenz, and L. Novotny, *Appl. Phys. Lett*. 77, 3459 (2000).

[11] E. H. Synge, "A Suggested Method For Extending Microscopic Resolution Into The Ultra-Microscopic Region," *Phil. Mag*., vol. 6, pp. 356--362, (1928).

[12] D. W. Pohl, W. Denk, and M. Lanz, "Optical Stethoscopy: Image Recording with Resolution λ/20," *Appl. Phys. Lett*., vol. 44, no. 7, pp. 651--653, (1984).

[13] E. Betzig, A. Lewis, A. Harootunian, M. Isaacson, and E. Kratschmer, "Near-field Scanning Optical Microscopy (NSOM): Development and Biophysical Applications," *Biophys. J*., vol. 49, pp. 268--279, (1986).

[14] J. W. P. Hsu, "Near-field Scanning Optical Microscopy of Electronic and Photonic Materials and Devices," *Mat. Sci. Engr*. Vol. 33(1), pp.1-50 (2001).

[15] K. Karrai and R. D. Grober, "Piezoelectric Tip-Sample Distance Control for Near Field Optical Microscopes," *Appl. Phys. Lett*., vol. 66, no. 14, pp. 1842--1844, 1995.